Electronic Supplementary Material (ESI) for Journal of Materials Chemistry B.
This journal is © The Royal Society of Chemistry 2020

Supporting Information

Hydrogels toughened by biominerals providing energy-dissipative sacrificial bonds

Kazuki Fukao,[a] Kazuki Tanaka,[a] Ryuji Kiyama,[a] Takayuki Nonoyama*[b,c] and Jian Ping Gong*[b,c,d]

[a] Graduate School of Life Science, Hokkaido University, Sapporo, 001-0021, Japan

[b] Faculty of Advanced Life Science, Hokkaido University, Sapporo, 001-0021, Japan

[c] Global Station for Soft Matter, Global Institution for Collaborative Research and Education (GI-CoRE), Hokkaido University, Sapporo, 001-0021, Japan

[d] Institute for Chemical Reaction Design and Discovery (WPI-ICReDD), Hokkaido University, Sapporo, 001-0021, Japan

*Corresponding author

E-mail: nonoyama@sci.hokudai.ac.jp (T. Nonoyama)

E-mail: gong@sci.hokudai.ac.jp (J.P. Gong)

Materials & Methods

Materials. *N,N*-dimethylacrylamide (DMAAm), *N,N'*-methylenebisacrylamide (MBAA), *N,N,N',N'*-tetramethylenediamine (TEMED), 2-oxoglutaric acid (α-keto), tris(hydroxymethyl)aminomethane (Tris buffer), calcium chloride ($CaCl_2$), dipotassium phosphate (K_2HPO_4) and 37% hydrochloric acid (HCl) were purchased from FUJIFILM Wako Pure Chemical Corporation, Inc. (Japan). Potassium persulfate (KPS) was purchased from Kanto chemical corporation, Inc. (Japan). Glass plates (FL3, 3 mm thickness) were purchased from AGC Inc. (Japan). London Resin (LR) white was purchased from Okenshoji Co., Ltd. (Japan). The gel precursor and mineralization solutions were prepared with distilled water. All the chemicals, except DMAAm, were used without further purification. DMAAm was used after vacuum distillation.

Synthesis of HAp-polymer double network (HAp/DN) hydrogel

1. PDMAAm gel as substrate for subsequent HAp crystallization. The PDMAAm gel was synthesized by radical polymerization from aqueous solution. This solution contained 1 M DMAAm as a monomer, 2 mol% MBAA as a cross-linker, and 0.1 mol% KPS and 1.0×10^{-4} vol% TEMED as initiators. The solution was injected into a mold consisting of a pair of glass plates separated by a 1.0 mm-thick silicone rubber. The PDMAAm gel was synthesized at room temperature for about 8 h under argon gas.

2. HAp mineralization to convert from soft PDMAAm network to brittle first network. To obtain HAp/SN gel, HAp was then mineralized in the presence of obtained PDMAAm hydrogel by the alternative soaking method.[1,2] First, the PDMAAm gel was immersed in 1 M Tris buffer solution (pH 9.0) to adjust pH of gels for 2 h because HAp is the most stable in the pH=8-9.[3] The PDMAAm gel was immersed in large amount of 300 mM K_2HPO_4 aq (pH 9.0) at room temperature for 110 s. The

gel was then washed by distilled water for 10 s to remove excess phosphate ions at gel surface. The gel was immersed in 500 mM $CaCl_2$ aq (pH 9.0) for 110 s, and rinsed for 10 s again. This alternative immersing process was repeated for n cycles (n = 0, 1, 3, 5 and 7) to mineralize calcium phosphate in the gel. After the alternative immersing, the PDMAAm gel was immersed in 500 mM $CaCl_2$ aqueous solution (pH 11) at 35 ℃ over 1 day to ripen the mineralized amorphous calcium phosphate (ACP) to HAp. To evaluate the effect of crystallinity of mineralized HAp, the ripening temperature T_r after the alternative immersing was controlled from room temperature to 80 ℃.

3. Introduction of soft second network into the first brittle gel. To obtain the HAp/DN gel, the HAp/SN gel was immersed in distilled water to remove excess calcium ions for 1 day. The HAp/SN gel was then immersed in an aqueous solution containing 2 M DMAAm, 0.2 mol% MBAA, and 0.1 mol% KPS for 1 day until reaching equilibrium. The sample was sandwiched between two glass plates, and polymerized again by heating at 60 ℃ for 8 h under air. The obtained HAp/DN gel was immersed in a distilled water pool for exchanging to fresh one to remove any unreacted chemicals. For samples to evaluate the effect of crystallinity of mineralized HAp, the HAp/SN gel was then immersed in an aqueous solution containing 2 M DMAAm, 0.2 mol% MBAA, and 0.1 mol% α-keto for 1 day, and UV polymerization was performed to avoid the influence of the temperature on the crystallinity during polymerization.

Material Characterization

X-ray diffraction (XRD). The crystal phase of mineralized calcium phosphate was evaluated by XRD spectrometry (Ultima IV, Rigaku, Japan). The extraction wavelength and output power of the X-rays generated by the Cu cube were 1.5406 Å and 0.8 kW (40 kV and 20 mA), respectively. The range of diffraction angle 2θ was from 10° to 60° at a scanning rate of 5 °/min and

from 20° to 35° at a scanning rate of 1.5 °/min.

Thermogravimetric/differential thermal analysis (TG/DTA). The weight fraction of mineral in HAp/DN gels was evaluated by using a thermogravimetric analyser (TG820 Thermo plus EVO, Rigaku). HAp/DN gel of several dozen milligrams were loaded in a platinum open pan, and the weight and differential thermal (DT) were measured from 30 to 600 °C at a heating rate of 10 °C/min. The weight fraction of HAp was determined from the weight of the final residue at 600 °C divided by the initial weight of loaded gel.

Field emission transmission electron microscopy (FE-TEM). The morphology of HAp in the HAp/DN gel (n=5) before and after stretching (λ = 2) was evaluated by FE-TEM (JEM-2100F, JEOL, Japan). To observe the morphology of HAp in stretching state of the gel, the HAp/DN gel was stretched by a self-made stretching device. The water in the stretched hydrogel was firstly exchanged with ethanol and then exchanged with acrylic resin (LR white). The solidification was done by thermal polymerization at 60 ^{o}C in overnight. Approximately 100-nm thick sections of the solidified samples were created by an ultra-microtome with diamond knife (EM UC7i, Leica Microsystems, Germany) and were placed on a copper mesh TEM grid. The acceleration voltage of the electron gun for observation was 200 kV. Selected area two-dimensional fast Fourier transformation (SA-2DFFT) was applied to high magnification image. The crystallinity was evaluated from the crystal lattice obtained by the Fourier transformation image using image J (v1.49).

Mechanical properties of HAp/DN gel

Tensile test. Uniaxial tensile test was carried out by using commercial tensile tester (Instron 5965, Instron Co., USA). Samples were cut into dumbbell shape with International Standard size ISO

37-2 (12 mm gauge length and 2 mm width). The test was performed at 100 mm/min of tensile speed and room temperature.

Cyclic test and separation of the total dissipative energy to polymer and HAp contributions. To estimate the energy dissipation during stretching, we conducted cyclic loading-unloading test. Sample size was same with that in tensile test. The gel was stretched up to λ=2 and then was unloaded to initial displacement at 100 mm/min by using Instron 5965. The total dissipated energy, E_{total}, of HAp/DN gel was estimated from the hysteresis area enclosed by loading-unloading curve. We assumed that this total dissipated energy possibly comes from three contributions, rupture of polymer, rupture of HAp, and debonding of polymer-HAp interface.

$$E_{total} = E_p + E_{HAp} + E_{p\cdot HAp} \quad \text{(S1)}$$

where E_p, E_{HAp} and $E_{p\cdot HAp}$ are polymer rupture energy, HAp rupture energy and debonding energy between polymer and HAp surface, respectively. To separate the E_{total} into E_p, E_{HAp} *and* $E_{p\cdot HAp}$, we used the methods illustrated in **Fig. S3**. To estimate $E_{p\cdot HAp}$, which is due to physical interactions, we measured the self-recovery of the stress -stretch ratio curve. We found that the first unloading curves and second loading curves with different waiting times (0 and 30 min) during the cyclic test were overlapped (**Fig. S2**), indicating that the hysteresis curves were irreversible. Accordingly, $E_{p\cdot HAp}$ was almost zero. To estimate E_p, we first prepared two samples that were non-stretched HAp/DN gel and

pre-stretched HAp/DN gel stretched up to λ=2. And then, both samples were immersed in HCl solution (3.5 wt%) for 1 min to dissolve HAp mineral. We confirmed that the acidic treatment did not damage the polymer network, as no differences in volume and in mechanical hysteresis were observed for the water-equilibrated sample and HCl-treated sample (**Fig. S4**). The non-stretched gel should have non-damaged polymer network, while the pre-stretched one might have damaged polymer network when during the pre-stretch. By comparing the stress-stretch ratio curves of the two samples, we can quantitatively estimate the damage of the polymer in the pre-stretched sample. The difference in the area enclosed by two loading curves is therefore the E_p, as schematically illustrated in **Fig. S3**.

Mechanism of energy dissipation owing to HAp

Wide angle X-ray diffraction (WAXD) of wet state HAp-DN gel. The 2-dimensional orientation of HAp was evaluated by high-brightness synchrotron X-ray facility of beam line BL05XU in SPring-8 (Hyogo, Japan). The extraction wavelength of synchrotron X-ray, the camera length of the distance between sample and detector and duration time were 1 Å (12.4 keV in energy), 0.15 m and 1 s, respectively. The stretching axis was set in parallel to the equatorial direction.

Analysis of anisotropy of mineralized HAp. To evaluate anisotropy of mineralized HAp, we calculated orientation degree from WAXD patterns. The intensities of water profile were much

higher than those of HAp in the raw 2D WAXD images. To isolate HAp diffraction profile, we subtracted the 2D profile of pristine interpenetrating network (IPN) gel from that of HAp/DN gel by image calculator processing on Image J (v1.49) software. The azimuthal angle φ starts from east direction in 2D image to the north in 2D images. We integrated the intensities in azimuthal angle φ = 70 °−110 ° and φ = 160 °−200 ° for outputting perpendicular and parallel 1D profiles to the stretching direction, respectively, by using Fit_2D (v12.077) software. To calculate quantitative orientation degree, the azimuthal angle distribution of HAp (002) plane was drawn from the isolated 2D profile. The orientation degree was calculated according to Herrmann's orientation function, *S*, as follows.[4]

$$S = \frac{3\langle \cos^2 \varphi \rangle - 1}{2} \; (-0.5 \leq S \leq 1) \tag{S2}$$

$$\langle \cos^2 \varphi \rangle = \frac{\int_0^{\pi/2} I(\varphi,002)\cos^2 \varphi \sin \varphi d\varphi}{\int_0^{\pi/2} I(\varphi, 002)\sin \varphi d\varphi} \tag{S3}$$

where $I(\varphi, 002)$ was intensity of (002) plane. For calculation of *S*, the range of φ was from 0 ° to 90 °. Here, $-0.5 \leq S < 0$, $S = 0$ and $0.5 < S \leq 1$ indicated parallel, random and perpendicular orientations against the stretching direction, respectively. -0.5 and 1 mean perfectly parallel and perpendicular orientations, respectively. Deconvolution of dense peak around 32° was performed by fitting the five peaks using the empirical peak shape function, $V(x)$, called as mixed Gaussian-Lorentzian function (pseudo-Voigt function) as follows (**Fig.S5**).[5]

$$V(x) = (1-\eta) \times \frac{2I}{H}\left(\frac{\ln 2}{\pi}\right)^{\frac{1}{2}} exp\left\{-4\ln 2\left(\frac{(x-x_0)}{H}\right)^2\right\} + \eta \times \frac{2I}{\pi H}\left\{1+\left(\frac{2(x-x_0)}{H}\right)^{-1}\right\} \quad \text{(S4)}$$

Where η, I, H, x and x_0 were the Lorentz fraction (η=0.9), the density index, the full width at half maximum (FWHM), the diffraction angle, 2θ, and the peak top position of each fitted peak, respectively.

Influence of the crystallinity of mineralized HAp. To evaluate the influence of the crystallinity of HAp on toughness of the HAp/DN (n=5) gel, we performed tensile test and cyclic test of samples with different HAp crystallinities. The crystallinity of HAp was controlled by changing the ripening temperature of mineralization, T_r, then we measured XRD to analyze crystallinity of mineralized HAp. To evaluate the crystallinity of mineralized HAp, we conducted curve fitting for the peak of (002) plane by using Igor Pro 7 (64-bit) software, and we defined the simple crystallinity of mineralized HAp as the ratio of the full width at half maximum (FWHM) relative to T_r = 25 ℃. We carried out cyclic test to evaluate the dissipated energy.

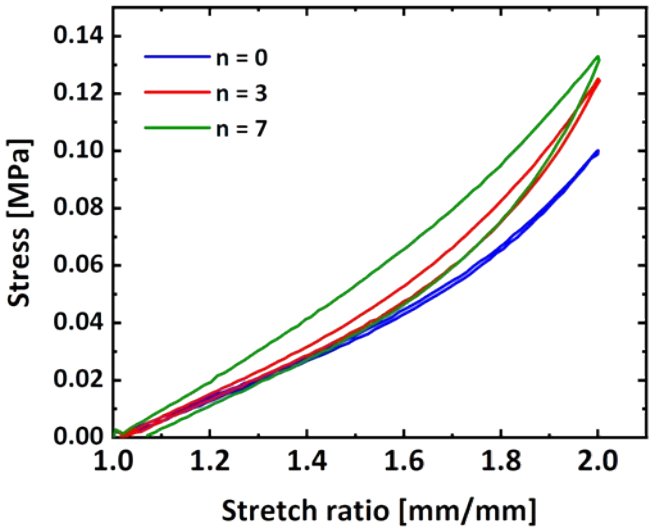

Fig. S1 Cyclic tests of HAp/DN gels (n=0 (blue), 3 (red) and 7 (green)). The hysteresis loss increases with *n* that has elevate weight fraction of mineralized HAp.

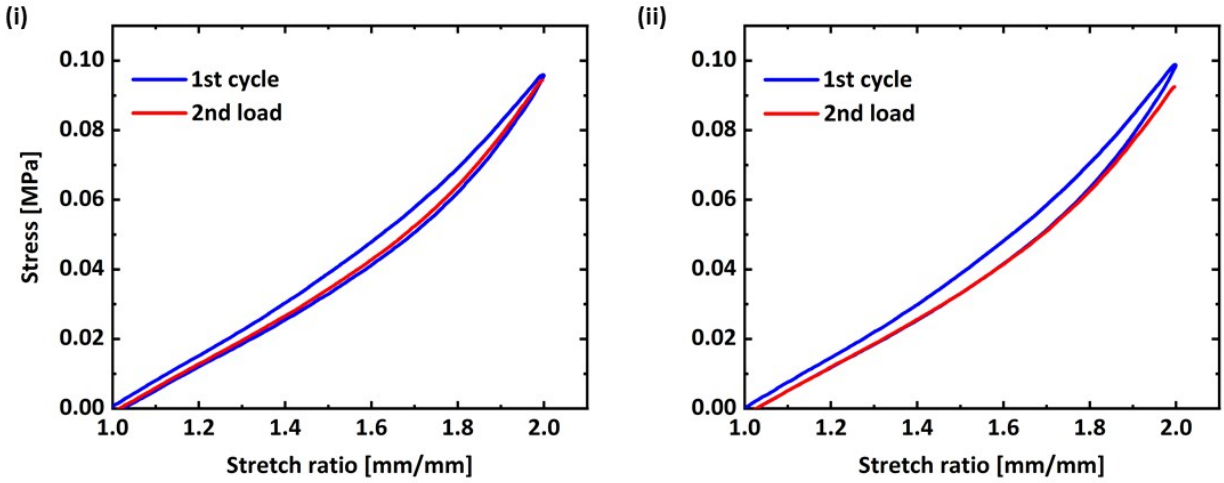

Fig. S2 Cyclic tests of HAp/DN gels (n = 5) with different waiting time during the cyclic test. Blue line is first load-unload curve, and red line is second load curve after waiting from first load-unload for (i) 0 min, (ii) 30 min. The second loading curve almost overlaps with the first unloading curve, indicating no self- recovery. From these results, the contribution of energy dissipation E_p due to the interfacial debonding between polymer chain and HAp crystal is negligible.

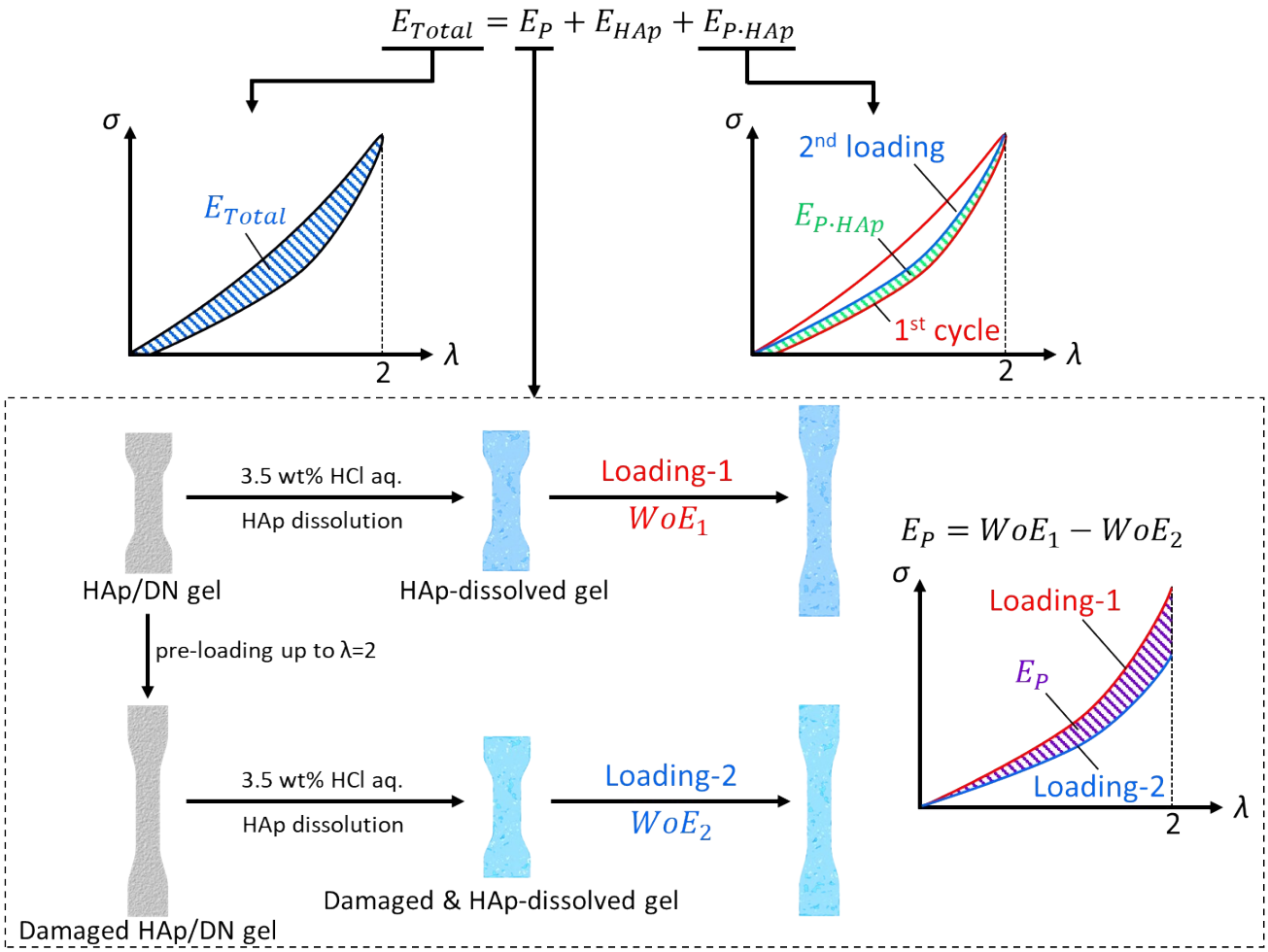

Fig. S3 Schematic explanation of how to separate the E_{Total} into E_P, E_{HAp} and $E_{p\cdot HAp}$.

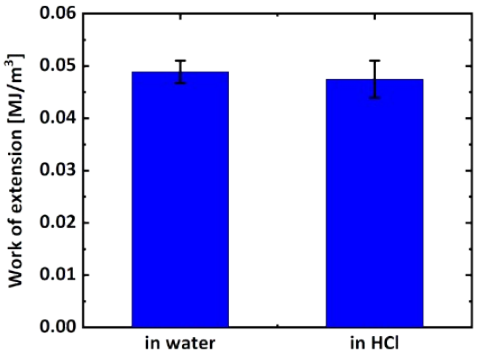

Fig. S4 Structure stability of PDAAm network in HCl aqueous solution (3.5 wt%) for 1 min. Work of extension of water-equilibrated and HCl-treated PDAAm gels are shown.

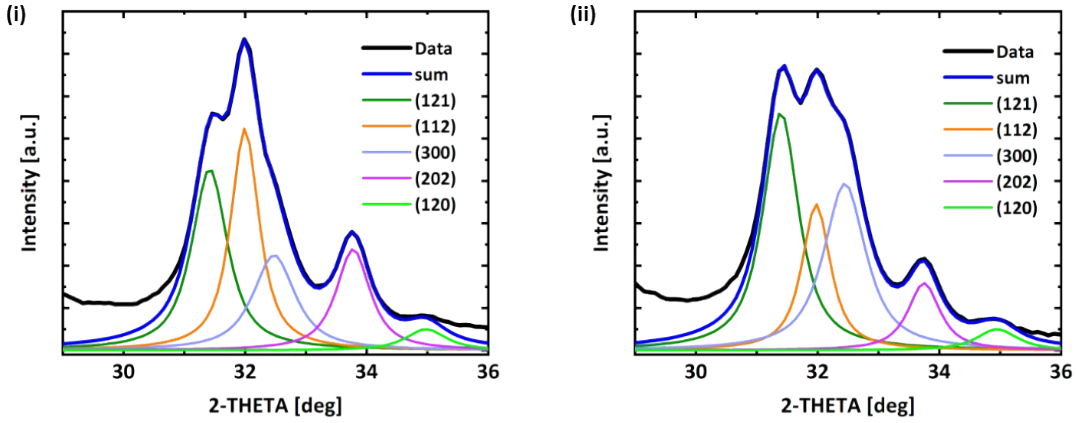

Fig. S5 Deconvolutions of the strong peak around 2-THETA = 32° into individual HAp peaks on the 1D profiles of stretched HAp/DN gel (n=5) in parallel (i) and perpendicular (ii) directions. The intensity of these separated peaks shows the c-axis orientation of mineralized HAp along with the stretch direction.

References

1 J. C. Góes, S. D. Figueiró, A. M. Oliveira, A. A. M. Macedo, C. C. Silva, N. M. P. S. Ricardo and A. S. B. Sombra, *Acta Biomaterialia*, 2007, **3**, 773–778.

2 R. Kiyama, T. Nonoyama, S. Wada, S. Semba, N. Kitamura, T. Nakajima, T. Kurokawa, K. Yasuda, S. Tanaka and J. P. Gong, *Acta Biomaterialia*, 2018, **81**, 60–69.

3 M. Kikuchi, T. Ikoma, S. Itoh, H. N. Matsumoto, Y. Koyama, K. Takakuda, K. Shinomiya and J. Tanaka, *Composites Science and Technology*, 2004, **64**, 819–825.

4 K. Fukao, T. Nonoyama, R. Kiyama, K. Furusawa, T. Kurokawa, T. Nakajima and J. P. Gong, *ACS Nano*, 2017, **11**, 12103–12110.

5 S. N. Kane, A. Mishra and A. K. Dutta, *Journal of Physics: Conference Series*, 2016, **755**, 6–10.